Near-field Tracking with Large Antenna Arrays: Fundamental Limits and Practical Algorithms

A. Guerra[⋆], F. Guidi[⋄], D. Dardari[⋆], P. M. Djurić[†]

[⋆]University of Bologna, UNIBO, Italy; [⋄]National Research Council, IEIIT, Italy

[†]Stony Brook University, SBU, USA.

STONY BROOK UNIVERSITY

ALMA MATER STUDIORUM
UNIVERSITÀ DI BOLOGNA

National Research Council of Italy

IEEE ICASSP 2022 Int. Conf. Acoustics, Speech, and Signal Process.

Outline

- Research Motivations
- Near-Field State-Space Model
- Posterior CRLB
- Tracking Algorithms
- Simulation Results
- Conclusions

Research Motivations

◇ Next 5G and 6G are pushing towards millimeter-wave and THz frequencies;

◇ The use of such high frequencies allows to pack a large number of antennas into a small area;

◇ The adoption of electrically large antenna arrays is such that the TX can be located in the near-field radiating (Fresnel) region of the RX (and not in far-field), even for large TX-RX distances.

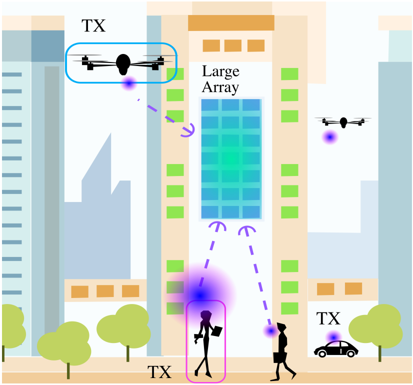

Fresnel Region

$$0.62\sqrt{\frac{D^3}{\lambda}} \leq d \leq d_{\mathsf{F}} = \frac{2\,D^2}{\lambda}$$

Research Motivations – Curvature-of-Arrival (COA)

- Curvature of arrival of the wavefront impinging on a large array when the source is in near–field in $\mathbf{p}_1$.
- When instead the source is in far–field in $\mathbf{p}_2$, the wavefront can be approximated as planar.

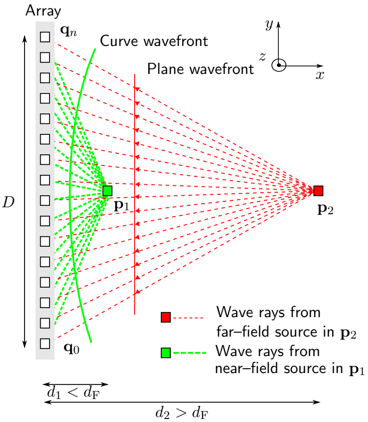

Research Motivations – COA for Source Tracking

- Source tracking with antenna arrays usually considers the joint estimate of angle-of-arrival (AOA) and time-of-arrival (TOA);

- Unfortunately, such an estimate requires a **fine synchronization** between the transmitter and receiver;
  - Traditional Solutions: Time difference-of-arrival (TDOA) or two-way ranging (TWR) approaches → need of an **exchange of messages** between nodes;

- In near-field it is possible to infer the source position directly from the **curvature-of-arrival** (COA) of the impinging spherical wavefront;

- Advantages of near-field localization:
  - only a **single antenna array** is sufficient to infer the user's position;
  - **no time or phase synchronization** is required between the user and the anchor.

Research Motivations – COA for Source Tracking

- Source tracking with antenna arrays usually considers the joint estimate of angle-of-arrival (AOA) and time-of-arrival (TOA);
- Unfortunately, such an estimate requires a **fine synchronization** between the transmitter and receiver;
  - Traditional Solutions: Time difference-of-arrival (TDOA) or two-way ranging (TWR) approaches → need of an **exchange of messages** between nodes;
- In near-field it is possible to infer the source position directly from the **curvature-of-arrival** (COA) of the impinging spherical wavefront;
- Advantages of near-field localization:
  - only a **single antenna array** is sufficient to infer the user's position;
  - **no time or phase synchronization** is required between the user and the anchor.

Research Motivations – COA for Source Tracking

- ◇ Source tracking with antenna arrays usually considers the joint estimate of angle-of-arrival (AOA) and time-of-arrival (TOA);
- ◇ Unfortunately, such an estimate requires a **fine synchronization** between the transmitter and receiver;
  - Traditional Solutions: Time difference-of-arrival (TDOA) or two-way ranging (TWR) approaches → need of an **exchange of messages** between nodes;
- ◇ In near-field it is possible to infer the source position directly from the **curvature-of-arrival** (COA) of the impinging spherical wavefront;
- ◇ Advantages of near-field localization:
  - only a **single antenna array** is sufficient to infer the user's position;
  - **no time or phase synchronization** is required between the user and the anchor.

Research Motivations – COA for Source Tracking

- Source tracking with antenna arrays usually considers the joint estimate of angle-of-arrival (AOA) and time-of-arrival (TOA);
- Unfortunately, such an estimate requires a **fine synchronization** between the transmitter and receiver;
  - Traditional Solutions: Time difference-of-arrival (TDOA) or two-way ranging (TWR) approaches $\rightarrow$ need of an **exchange of messages** between nodes;
- In near-field it is possible to infer the source position directly from the **curvature-of-arrival** (COA) of the impinging spherical wavefront;
- Advantages of near-field localization:
  - only a **single antenna array** is sufficient to infer the user's position;
  - **no time or phase synchronization** is required between the user and the anchor.

Outline

- Research Motivations
- Near-Field State-Space Model
- Posterior CRLB
- Tracking Algorithms
- Simulation Results
- Conclusions

State–Space Model - System Geometry

- The goal of the tracking problem is to estimate the state of a target, that is $\mathbf{s}_k = \left[\mathbf{p}_k^\mathsf{T},\, \mathbf{v}_k^\mathsf{T}\right]^\mathsf{T}$ given the history of measurements up to time instant k.
- The array antenna coordinates are indicated with $\mathbf{q}_n = [x_n,\, y_n,\, z_n]^\mathsf{T}$, $n \in \mathcal{N} = \{0, \ldots, N-1\}$.

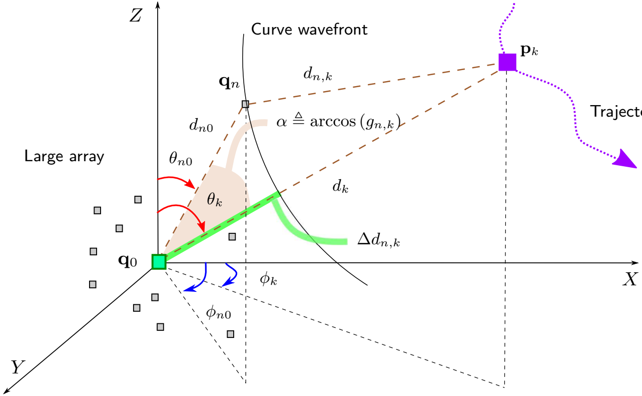

State–Space Model - Signal Model

◇ The received signal at the nth antenna of the array is

$$r_n(t) = a_{n,k} \cos(2\pi f_p t - \vartheta_{n,k}) + \nu_{n,k}(t),$$

↪ $a_{n,k} \triangleq \dfrac{A\lambda}{4\pi d_{n,k}}$: signal amplitude with λ being the signal wavelength, and $d_{n,k} = \|\mathbf{p}_k - \mathbf{q}_n\|_2$ is the target-antenna distance;

↪ $\vartheta_{n,k} \triangleq 2\pi f_p \left(\dfrac{d_{n,k}}{c} + t_0\right)$: signal phase with t_0 being a clock offset;

↪ The phase-difference is $\Delta\vartheta_{n,k} \triangleq \dfrac{2\pi}{\lambda} \Delta d_{n,k}$, with $\Delta d_{n,k} \triangleq d_{n,k} - d_k$;

↪ $\nu_{n,k}(t)$ is the signal noise modeled as AWGN with double-sided power spectral density $N_0/2$.

State–Space Model

- The sequential state estimation problem (tracking) can be formulated starting from a discrete-time state-space representation given by

$$\mathbf{s}_k = \mathbf{s}_k^- + \mathbf{w}_k = \mathbf{A}_k \, \mathbf{s}_{k-1} + \mathbf{w}_k,$$
$$\mathbf{z}_k = h\left(\mathbf{p}_k\right) + \boldsymbol{\eta}_k,$$

  - ↪ $\mathbf{A}$: Transition matrix; $\mathbf{w}_k \sim \mathcal{N}\left(\mathbf{w}_k; \mathbf{0}, \mathbf{Q}\right)$ is the zero-mean noise process where $\mathbf{Q}$ is the transition noise covariance matrix;
  - ↪ The expected observation at the nth antenna of the ℓth array is

$$h\left(\mathbf{p}_k\right) = \Delta\vartheta_{n,k} \mod 2\pi,$$

  - ↪ The observation noise process is modeled as $\boldsymbol{\eta}_k \sim \mathcal{N}\left(\boldsymbol{\eta}_k; \mathbf{0}, \mathbf{R}_k\right)$ where $\mathbf{R}_k$ is a diagonal matrix whose generic element is given by var$\left(\Delta\vartheta_{n,k}\right)$.

State–Space Model - Near-Field Observation Model

◇ The curvature of the impinging wave is encapsulated in the measurement model as

$$h(\mathbf{p}_k) \propto \Delta d_{n,k}(\mathbf{q}_n, \mathbf{p}_k) = d_k \left[\sqrt{\mathrm{f}_{n,k}} - 1\right],$$

$$\mathrm{f}_{n,k} \triangleq \mathrm{f}_{n,k}(\mathbf{q}_n, \mathbf{p}_k) = 1 + \left(\frac{d_{n0}}{d_k}\right)^2 - 2\frac{d_{n0}}{d_k}\, g_{n,k},$$

↪ **Definitions.** Inter-antenna distances: $d_{n0} = \|\mathbf{q}_n - \mathbf{q}_0\|_2$, Target-array distance: $d_k = \|\mathbf{q}_0 - \mathbf{p}_k\|_2$; Angular term: $g_{n,k} = \sin(\theta_{n0})\sin(\theta_k)\cos(\phi_{n0} - \phi_k) + \cos(\theta_{n0})\cos(\theta_k)$;

↪ **Near–field Model.** $\dfrac{d_{n0}}{d_k} \gg 1$: near-field model $\rightarrow \mathrm{f}_{n,k} \gg 1$ curvature of the impinging wavefront with ranging and bearing information.

Outline

- ◇ Research Motivations
- ◇ Near-Field State-Space Model
- ◇ Posterior CRLB
- ◇ Tracking Algorithms
- ◇ Simulation Results
- ◇ Conclusions

Posterior CRLB - PCRB

◇ Derivation of the P-CRLB to assess the ultimate performance of the COA–based tracking in the near– and far–field regions;

The FIM of $\mathbf{s}_k$ can be recursively computed as [Tichavsky, Muravchik, Nehorai, 1998]

$$\mathbf{J}_k = \mathbf{D}_{k-1}^{22} - \mathbf{D}_{k-1}^{21} \left(\mathbf{J}_{k-1} + \mathbf{D}_{k-1}^{11}\right)^{-1} \mathbf{D}_{k-1}^{12} \,,$$

where $\mathbf{D}_{k-1}^{11} = \mathbf{A}^{\mathsf{T}}\mathbf{Q}^{-1}\mathbf{A}$, $\mathbf{D}_{k-1}^{12} = \mathbf{D}_{k-1}^{21} = -\mathbf{A}^{\mathsf{T}}\mathbf{Q}^{-1}$, $\mathbf{D}_{k-1}^{22} = \mathbf{Q}^{-1} + \mathbf{J}_k^{\mathrm{D}}$ where $\mathbf{J}_k^{\mathrm{D}}$ is the expectation of the Hessian matrix, i.e.,

$$\mathbf{J}_k^{\mathrm{D}} = \mathbb{E}_{\mathbf{s}_k|\mathbf{s}_{k-1}} \left\{\mathbb{E}_{\mathbf{z}_k|\mathbf{s}_k} \left\{-\Delta_{\mathbf{s}_k}^{\mathbf{s}_k} \ln p\left(\mathbf{z}_k|\mathbf{s}_k\right)\right\}\right\} = \mathbb{E}_{\mathbf{s}_k|\mathbf{s}_{k-1}} \left\{\tilde{\mathbf{J}}_k^{\mathrm{D}}\right\},$$

with $\tilde{\mathbf{J}}_k^{\mathrm{D}}$ being the non-Bayesian data FIM.

◇ Analysis of the FIMs on ranging and bearing information and their asymptotic behaviors for three different array geometries.

Posterior CRLB - PCRB

- Derivation of the P-CRLB to assess the ultimate performance of the COA–based tracking in the near– and far–field regions;
  - Analysis of the FIMs on ranging and bearing information and their asymptotic behaviors for three different array geometries.

FIMs for UCA and Source on CPL

The FIMs for a UCA on the YZ-plane and a target on the X-axis are

$$\tilde{J}^{\mathrm{D}}(d) = \frac{4\,N\,\pi^2}{\lambda^2\,\sigma_\eta^2} \cdot \frac{2 + \frac{D^2}{4\,d^2} - 2\sqrt{1 + \frac{D^2}{4\,d^2}}}{1 + \frac{D^2}{4\,d^2}},$$

$$\tilde{J}^{\mathrm{D}}(\theta) = \tilde{J}^{\mathrm{D}}(\phi) = \frac{N\,\pi^2}{2\,\lambda^2\sigma_\eta^2}\,\frac{D^2}{1 + \frac{D^2}{4\,d^2}}.$$

Posterior CRLB - PCRB

- Derivation of the P-CRLB to assess the ultimate performance of the COA–based tracking in the near– and far–field regions;

  - Analysis of the FIMs on ranging and bearing information and their asymptotic behaviors for three different array geometries.

FIMs for UCA and Source on CPL and in Far–Field

For $d_k \gg d_{\mathrm{F}}$ (far–field region), we get

$$\tilde{J}^{\mathrm{D}}\left(d\right) = 0,$$

$$\tilde{J}^{\mathrm{D}}\left(\theta\right) = \tilde{J}^{\mathrm{D}}\left(\phi\right) = \frac{D^2\, N\, \pi^2}{2\, \lambda^2 \sigma_\eta^2}.$$

Posterior CRLB - Results

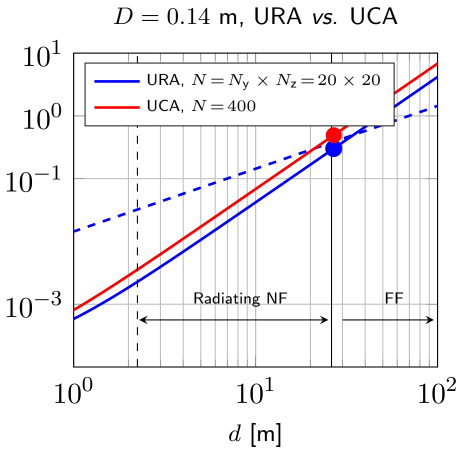

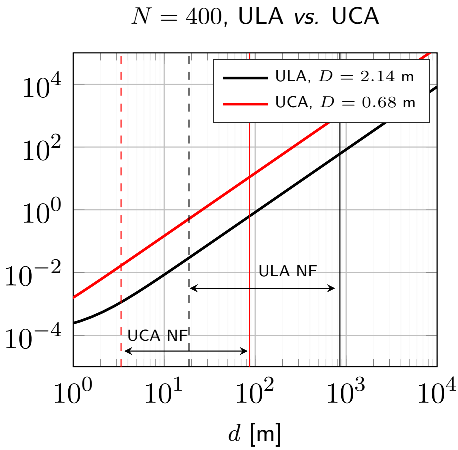

Ranging error $\sqrt{\left[\tilde{J}^{\mathrm{D}}(d)\right]^{-1}}$ as a function of the source distance d and different array geometries. We set $f_p = 28$ GHz and $\sigma_\eta = 20^\circ$. The threshold, indicated with a dashed line, corresponds to ranging error of $1/10$ of the actual distance.

Outline

- Research Motivations
- Near-Field State-Space Model
- Posterior CRLB
- Tracking Algorithms
- Simulation Results
- Conclusions

Tracking Algorithms

- We tested different tracking algorithms:
  - **Extended Kalman Filter**: for non-linear Gaussian state-space models

    ↪ It requires the linearization of the observation model:

$$\{\mathbf{H}_k\}_n = \nabla_{\mathbf{s}_k} h_n(\mathbf{p}_k) = \frac{2\pi}{\lambda} \nabla_{\mathbf{s}_k} \Delta d_{n,k}(\mathbf{p}_k),$$

  - **Particle Filter**: for arbitrary distribution functions described by a set of particles and weights $\{\mathbf{s}_{m,k}, w_{m,k}\}_{m=1}^{M}$

    ↪ It requires the design of the importance sampling (IS) function:

    - ⊗ Prior IS;
    - □ Likelihood IS;
    - ⋆ Linearised optimal IS.

Tracking Algorithms

◇ We tested different tracking algorithms:

- **Extended Kalman Filter**: for non-linear Gaussian state-space models

  ↪ It requires the linearization of the observation model:

$$\{\mathbf{H}_k\}_n = \nabla_{\mathbf{s}_k} h_n(\mathbf{p}_k) = \frac{2\pi}{\lambda} \nabla_{\mathbf{s}_k} \Delta d_{n,k}(\mathbf{p}_k),$$

- **Particle Filter**: for arbitrary distribution functions described by a set of particles and weights $\{\mathbf{s}_{m,k}, w_{m,k}\}_{m=1}^{M}$

  ↪ It requires the design of the importance sampling (IS) function:

  ⊗ Prior IS;
  ☐ Likelihood IS;
  ⋆ Linearised optimal IS.

Tracking Algorithms - IS Design

⊗ **PF - Prior IS**: Particles generation/propagation and weights are implemented as

$$\mathbf{s}_{m,k} \sim p\left(\mathbf{s}_{m,k} | \mathbf{s}_{m,k-1}\right) = \mathcal{N}\left(\mathbf{s}_{m,k}; \mathbf{A}\, \mathbf{s}_{m,k-1}, \mathbf{Q}\right),$$
$$w_{m,k} = w_{m,k-1}\, p\left(\mathbf{z}_k | \mathbf{s}_{m,k}\right).$$

☺ PFs work surprisingly well in most settings + low-complexity

☹ Particles are propagated without considering the newest measurements $\mathbf{z}_k$.

□ PF - Likelihood IS

⋆ PF - Linearised Optimal IS

Tracking Algorithms - IS Design

⊗ **PF - Prior IS**

☐ **PF - Likelihood IS**: Particles and weights are generated as

$$\mathbf{s}_{m,k} \sim \mathcal{N}\left(\mathbf{s}_{m,k}; \hat{\mathbf{s}}_{\mathsf{ML},k}, \mathbf{P}_{\mathsf{ML},k}\right) ,$$
$$w_{m,k} = w_{m,k-1} \frac{p\left(\mathbf{z}_k | \mathbf{s}_{m,k}\right) p\left(\mathbf{s}_{m,k} | \mathbf{s}_{m,k-1}\right)}{\mathcal{N}\left(\mathbf{s}_{m,k}; \hat{\mathbf{s}}_{\mathsf{ML},k}, \mathbf{P}_{\mathsf{ML},k}\right)} .$$

- ☺ Likelihood IS works well when the likelihood is more informative than the prior.
- ☹ It requires a maximum likelihood estimator.

⋆ **PF - Linearised Optimal IS**

Tracking Algorithms - IS Design

- ⊗ **PF - Prior IS**
- ☐ **PF - Likelihood IS**
- ⋆ **PF - Linearised Optimal IS**: A possible choice for the optimal IS is to directly sample from the posterior

$$\pi\left(\mathbf{s}_k \middle| \mathbf{s}_{m,k-1}, \mathbf{z}_k\right) = \frac{p\left(\mathbf{z}_k \middle| \mathbf{s}_k\right) p\left(\mathbf{s}_k \middle| \mathbf{s}_{m,k-1}\right)}{\int p\left(\mathbf{z}_k \middle| \mathbf{s}_k\right) p\left(\mathbf{s}_k \middle| \mathbf{s}_{m,k-1}\right) d\mathbf{s}_k},$$

where an analytical form can be found if the observation function is linear and the noises in the state and observation equations are Gaussians and additive.

Outline

- Research Motivations
- Near-Field State-Space Model
- Posterior CRLB
- Tracking Algorithms
- Simulation Results
- Conclusions

Simulation Results

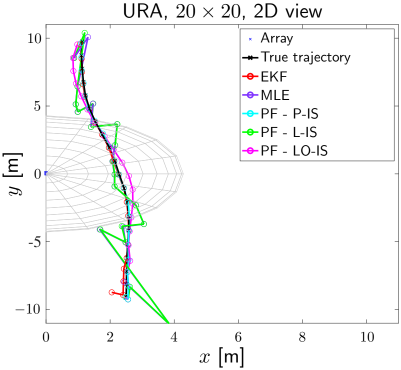

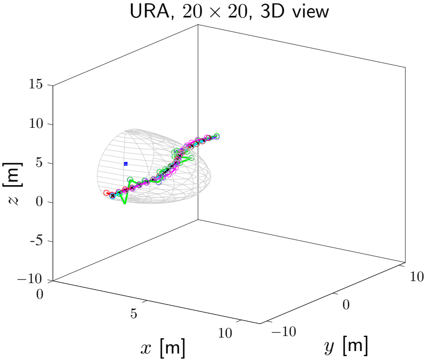

Example of estimated trajectories for different approaches and array sizes. URA with $N = 20 \times 20$ antennas, TM_0, MM_0; The array reference location is in $[0,\ 0,\ 1]$ and is lying in the YZ plane. (P-IS) indicates the PF with prior IS, (LO-IS) is the PF with linearised optimal IS and (L-IS) is the PF with likelihood IS.

Simulation Results

- Millimeter-wave antenna array ($f = 28\,$GHz). The number of particles was $M = 1000$, and the total number of time instants was $K = 20$;
- The array was planar, squared, with $N_\mathrm{y} = N_\mathrm{z} \in \{20,\, 30\}$;
- The initial state was $\mathbf{s}_0 = (2.5,\, -9.1,\, 1.5,\, 0.01,\, 0.97,\, 0)$;
- The actual transition of the source followed a linear model with

$$\mathbf{A} = \begin{bmatrix} \mathbf{I}_3 & \tau\,\mathbf{I}_3 \\ \mathbf{0}_3 & \mathbf{I}_3 \end{bmatrix}, \qquad \mathbf{Q} = \begin{bmatrix} \frac{\tau^3}{3}\mathbf{Q}_\mathrm{a} & \frac{\tau^2}{2}\mathbf{Q}_\mathrm{a} \\ \frac{\tau^2}{2}\mathbf{Q}_\mathrm{a} & \tau\,\mathbf{Q}_\mathrm{a} \end{bmatrix},$$

- $\mathbf{Q}_\mathrm{a} = \mathrm{diag}\left(\sigma^2_{\mathrm{a,x}}, \sigma^2_{\mathrm{a,y}}, \sigma^2_{\mathrm{a,z}}\right)$, with $\sigma^2_{\mathrm{a,x}} = \sigma^2_{\mathrm{a,y}} = \gamma_\mathrm{t}\, 0.03^2 \; \left(\mathrm{m}^2/\mathrm{step}^6\right)$, $\sigma^2_{\mathrm{a,z}} = 0$. We set $\gamma_\mathrm{t} = 1$ and $\gamma_\mathrm{t} = 10$, representing the possibility to work with transition parameter match (TM_0) or not (TM_1).
- The measurements noise standard deviation was set to $\sigma_\eta = \sigma \cdot (1 + \gamma_\mathrm{m})$ with $\sigma = 20^\circ$ and where $\gamma_\mathrm{m} = 0$ (i.e., $\sigma_\eta = 20^\circ$) and $\gamma_\mathrm{m} = 1$ (i.e., $\sigma_\eta = 40^\circ$) denote a measurement parameter match (MM_0) or mismatch (MM_1);
- EKF/PF Init: $\mathbf{m}_0 = \mathcal{N}\left(\mathbf{s}_0, \mathbf{P}_0\right)$ and $\mathbf{P}_0 = \mathrm{diag}\left(0.5^2, 0.5^2, 0.01^2, 10^{-6}, 10^{-2}, 0\right)$

Simulation Results

- Millimeter-wave antenna array ($f = 28\,$GHz). The number of particles was $M = 1000$, and the total number of time instants was $K = 20\,$;
- The array was planar, squared, with $N_{\mathsf{y}} = N_{\mathsf{z}} \in \{20,\, 30\}$;
- The initial state was $\mathbf{s}_0 = (2.5,\, -9.1,\, 1.5,\, 0.01,\, 0.97,\, 0)$;
- The actual transition of the source followed a linear model with

$$\mathbf{A} = \begin{bmatrix} \mathbf{I}_3 & \tau\,\mathbf{I}_3 \\ \mathbf{0}_3 & \mathbf{I}_3 \end{bmatrix}, \qquad \mathbf{Q} = \begin{bmatrix} \frac{\tau^3}{3}\mathbf{Q}_{\mathsf{a}} & \frac{\tau^2}{2}\mathbf{Q}_{\mathsf{a}} \\ \frac{\tau^2}{2}\mathbf{Q}_{\mathsf{a}} & \tau\,\mathbf{Q}_{\mathsf{a}} \end{bmatrix},$$

- $\mathbf{Q}_{\mathsf{a}} = \mathrm{diag}\left(\sigma^2_{\mathsf{a,x}}, \sigma^2_{\mathsf{a,y}}, \sigma^2_{\mathsf{a,z}}\right)$, with $\sigma^2_{\mathsf{a,x}} = \sigma^2_{\mathsf{a,y}} = \gamma_{\mathsf{t}}\, 0.03^2\, \left(\mathsf{m}^2/\mathsf{step}^6\right)$, $\sigma^2_{\mathsf{a,z}} = 0$. We set $\gamma_{\mathsf{t}} = 1$ and $\gamma_{\mathsf{t}} = 10$, representing the possibility to work with transition parameter match (TM_0) or not (TM_1).
- The measurements noise standard deviation was set to $\sigma_\eta = \sigma \cdot (1 + \gamma_{\mathsf{m}})$ with $\sigma = 20^\circ$ and where $\gamma_{\mathsf{m}} = 0$ (i.e., $\sigma_\eta = 20^\circ$) and $\gamma_{\mathsf{m}} = 1$ (i.e., $\sigma_\eta = 40^\circ$) denote a measurement parameter match (MM_0) or mismatch (MM_1);
- EKF/PF Init: $\mathbf{m}_0 = \mathcal{N}\left(\mathbf{s}_0, \mathbf{P}_0\right)$ and $\mathbf{P}_0 = \mathrm{diag}\left(0.5^2, 0.5^2, 0.01^2, 10^{-6}, 10^{-2}, 0\right)$

Simulation Results

- Millimeter-wave antenna array ($f = 28\,$GHz). The number of particles was $M = 1000$, and the total number of time instants was $K = 20$;
- The array was planar, squared, with $N_{\mathrm{y}} = N_{\mathrm{z}} \in \{20,\, 30\}$;
- The initial state was $\mathrm{s}_0 = (2.5,\, -9.1,\, 1.5,\, 0.01,\, 0.97,\, 0)$;
- The actual transition of the source followed a linear model with

$$\mathbf{A} = \begin{bmatrix} \mathbf{I}_3 & \tau\,\mathbf{I}_3 \\ \mathbf{0}_3 & \mathbf{I}_3 \end{bmatrix}, \qquad \mathbf{Q} = \begin{bmatrix} \frac{\tau^3}{3}\mathbf{Q}_{\mathrm{a}} & \frac{\tau^2}{2}\mathbf{Q}_{\mathrm{a}} \\ \frac{\tau^2}{2}\mathbf{Q}_{\mathrm{a}} & \tau\,\mathbf{Q}_{\mathrm{a}} \end{bmatrix},$$

- $\mathbf{Q}_{\mathrm{a}} = \mathrm{diag}\left(\sigma^2_{\mathrm{a,x}}, \sigma^2_{\mathrm{a,y}}, \sigma^2_{\mathrm{a,z}}\right)$, with $\sigma^2_{\mathrm{a,x}} = \sigma^2_{\mathrm{a,y}} = \gamma_{\mathrm{t}}\, 0.03^2 \,\left(\mathrm{m}^2/\mathrm{step}^6\right)$, $\sigma^2_{\mathrm{a,z}} = 0$. We set $\gamma_{\mathrm{t}} = 1$ and $\gamma_{\mathrm{t}} = 10$, representing the possibility to work with transition parameter match (TM_0) or not (TM_1).
- The measurements noise standard deviation was set to $\sigma_\eta = \sigma \cdot (1 + \gamma_{\mathrm{m}})$ with $\sigma = 20^\circ$ and where $\gamma_{\mathrm{m}} = 0$ (i.e., $\sigma_\eta = 20^\circ$) and $\gamma_{\mathrm{m}} = 1$ (i.e., $\sigma_\eta = 40^\circ$) denote a measurement parameter match (MM_0) or mismatch (MM_1);
- EKF/PF Init: $\mathbf{m}_0 = \mathcal{N}(\mathrm{s}_0, \mathbf{P}_0)$ and $\mathbf{P}_0 = \mathrm{diag}\left(0.5^2, 0.5^2, 0.01^2, 10^{-6}, 10^{-2}, 0\right)$

Simulation Results

- Millimeter-wave antenna array ($f = 28\,$GHz). The number of particles was $M = 1000$, and the total number of time instants was $K = 20$;
- The array was planar, squared, with $N_{\mathsf{y}} = N_{\mathsf{z}} \in \{20,\, 30\}$;
- The initial state was $\mathbf{s}_0 = (2.5,\, -9.1,\, 1.5,\, 0.01,\, 0.97,\, 0)$;
- The actual transition of the source followed a linear model with

$$\mathbf{A} = \begin{bmatrix} \mathbf{I}_3 & \tau\,\mathbf{I}_3 \\ \mathbf{0}_3 & \mathbf{I}_3 \end{bmatrix}, \qquad \mathbf{Q} = \begin{bmatrix} \frac{\tau^3}{3}\mathbf{Q}_{\mathsf{a}} & \frac{\tau^2}{2}\mathbf{Q}_{\mathsf{a}} \\ \frac{\tau^2}{2}\mathbf{Q}_{\mathsf{a}} & \tau\,\mathbf{Q}_{\mathsf{a}} \end{bmatrix},$$

- $\mathbf{Q}_{\mathsf{a}} = \mathrm{diag}\left(\sigma^2_{\mathsf{a,x}}, \sigma^2_{\mathsf{a,y}}, \sigma^2_{\mathsf{a,z}}\right)$, with $\sigma^2_{\mathsf{a,x}} = \sigma^2_{\mathsf{a,y}} = \gamma_{\mathsf{t}}\, 0.03^2\ \left(\mathsf{m}^2/\mathsf{step}^6\right)$, $\sigma^2_{\mathsf{a,z}} = 0$. We set $\gamma_{\mathsf{t}} = 1$ and $\gamma_{\mathsf{t}} = 10$, representing the possibility to work with transition parameter match (TM_0) or not (TM_1).
- The measurements noise standard deviation was set to $\sigma_\eta = \sigma \cdot (1 + \gamma_{\mathsf{m}})$ with $\sigma = 20^\circ$ and where $\gamma_{\mathsf{m}} = 0$ (i.e., $\sigma_\eta = 20^\circ$) and $\gamma_{\mathsf{m}} = 1$ (i.e., $\sigma_\eta = 40^\circ$) denote a measurement parameter match (MM_0) or mismatch (MM_1);
- EKF/PF Init: $\mathbf{m}_0 = \mathcal{N}\left(\mathbf{s}_0, \mathbf{P}_0\right)$ and $\mathbf{P}_0 = \mathrm{diag}\left(0.5^2, 0.5^2, 0.01^2, 10^{-6}, 10^{-2}, 0\right)$

Simulation Results

- Millimeter-wave antenna array ($f = 28$ GHz). The number of particles was $M = 1000$, and the total number of time instants was $K = 20$;
- The array was planar, squared, with $N_\mathsf{y} = N_\mathsf{z} \in \{20,\, 30\}$;
- The initial state was $\mathbf{s}_0 = (2.5,\, -9.1,\, 1.5,\, 0.01,\, 0.97,\, 0)$;
- The actual transition of the source followed a linear model with

$$\mathbf{A} = \begin{bmatrix} \mathbf{I}_3 & \tau\,\mathbf{I}_3 \\ \mathbf{0}_3 & \mathbf{I}_3 \end{bmatrix}, \qquad \mathbf{Q} = \begin{bmatrix} \frac{\tau^3}{3}\mathbf{Q}_\mathsf{a} & \frac{\tau^2}{2}\mathbf{Q}_\mathsf{a} \\ \frac{\tau^2}{2}\mathbf{Q}_\mathsf{a} & \tau\,\mathbf{Q}_\mathsf{a} \end{bmatrix},$$

- $\mathbf{Q}_\mathsf{a} = \mathrm{diag}\left(\sigma^2_{\mathsf{a,x}}, \sigma^2_{\mathsf{a,y}}, \sigma^2_{\mathsf{a,z}}\right)$, with $\sigma^2_{\mathsf{a,x}} = \sigma^2_{\mathsf{a,y}} = \gamma_\mathsf{t}\, 0.03^2\ \left(\mathsf{m}^2/\mathsf{step}^6\right)$, $\sigma^2_{\mathsf{a,z}} = 0$. We set $\gamma_\mathsf{t} = 1$ and $\gamma_\mathsf{t} = 10$, representing the possibility to work with transition parameter match (TM_0) or not (TM_1).
- The measurements noise standard deviation was set to $\sigma_\eta = \sigma \cdot (1 + \gamma_\mathsf{m})$ with $\sigma = 20^\circ$ and where $\gamma_\mathsf{m} = 0$ (i.e., $\sigma_\eta = 20^\circ$) and $\gamma_\mathsf{m} = 1$ (i.e., $\sigma_\eta = 40^\circ$) denote a measurement parameter match (MM_0) or mismatch (MM_1);
- EKF/PF Init: $\mathbf{m}_0 = \mathcal{N}(\mathbf{s}_0, \mathbf{P}_0)$ and $\mathbf{P}_0 = \mathrm{diag}\left(0.5^2, 0.5^2, 0.01^2, 10^{-6}, 10^{-2}, 0\right)$

Simulation Results

- Millimeter-wave antenna array ($f = 28\,\text{GHz}$). The number of particles was $M = 1000$, and the total number of time instants was $K = 20$;
- The array was planar, squared, with $N_\text{y} = N_\text{z} \in \{20,\ 30\}$;
- The initial state was $\mathbf{s}_0 = (2.5,\ -9.1,\ 1.5,\ 0.01,\ 0.97,\ 0)$;
- The actual transition of the source followed a linear model with

$$\mathbf{A} = \begin{bmatrix} \mathbf{I}_3 & \tau\,\mathbf{I}_3 \\ \mathbf{0}_3 & \mathbf{I}_3 \end{bmatrix}, \qquad \mathbf{Q} = \begin{bmatrix} \frac{\tau^3}{3}\mathbf{Q}_\text{a} & \frac{\tau^2}{2}\mathbf{Q}_\text{a} \\ \frac{\tau^2}{2}\mathbf{Q}_\text{a} & \tau\,\mathbf{Q}_\text{a} \end{bmatrix},$$

- $\mathbf{Q}_\text{a} = \operatorname{diag}\left(\sigma^2_{\text{a,x}}, \sigma^2_{\text{a,y}}, \sigma^2_{\text{a,z}}\right)$, with $\sigma^2_{\text{a,x}} = \sigma^2_{\text{a,y}} = \gamma_\text{t}\,0.03^2\ \left(\text{m}^2/\text{step}^6\right)$, $\sigma^2_{\text{a,z}} = 0$. We set $\gamma_\text{t} = 1$ and $\gamma_\text{t} = 10$, representing the possibility to work with transition parameter match (TM_0) or not (TM_1).
- The measurements noise standard deviation was set to $\sigma_\eta = \sigma \cdot (1 + \gamma_\text{m})$ with $\sigma = 20^\circ$ and where $\gamma_\text{m} = 0$ (i.e., $\sigma_\eta = 20^\circ$) and $\gamma_\text{m} = 1$ (i.e., $\sigma_\eta = 40^\circ$) denote a measurement parameter match (MM_0) or mismatch (MM_1);
- EKF/PF Init: $\mathbf{m}_0 = \mathcal{N}(\mathbf{s}_0, \mathbf{P}_0)$ and $\mathbf{P}_0 = \operatorname{diag}\left(0.5^2, 0.5^2, 0.01^2, 10^{-6}, 10^{-2}, 0\right)$

Simulation Results

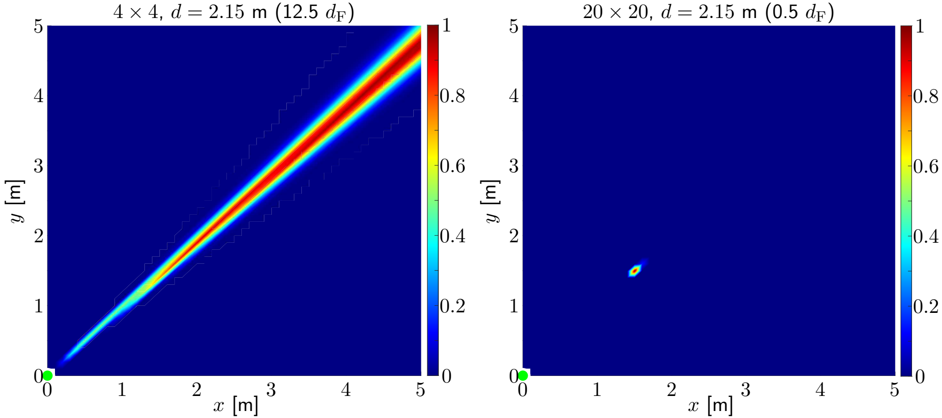

◇ Normalized LF for planar arrays with 4×4 (left) and 20×20 (right) antennas on the $YZ-$ plane, with $\sigma_\eta = 20^\circ$. The receiver and target locations were in $[0, 0, 1]$ (indicated as green markers) and in $[1.51,\ 1.51,\ 1]$.

Simulation Results

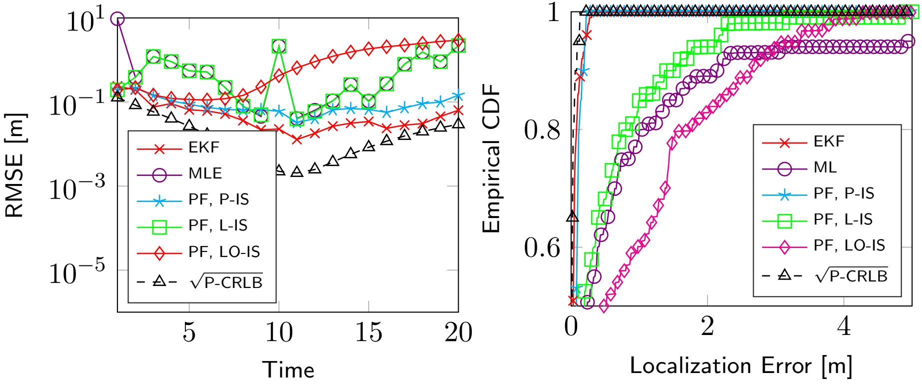

◇ RMSE (left) and Empirical CDF (right) vs. Localization error in meters for different estimators and by considering a URA with $N = 30 \times 30$ antennas, respectively. The measurement noise variance is set to $\sigma_\eta = 20^\circ$.

Simulation Results

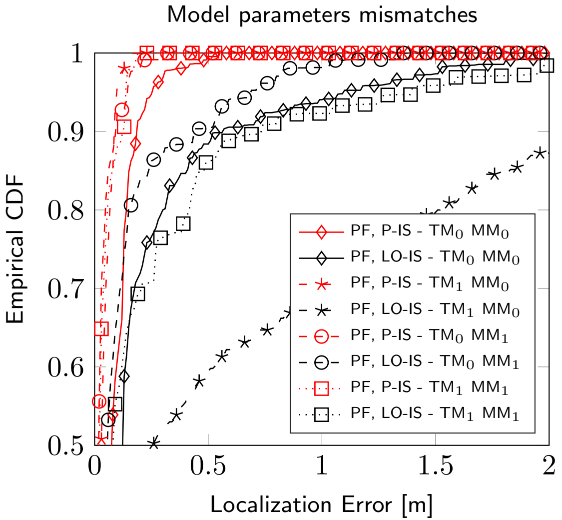

Simulation Results

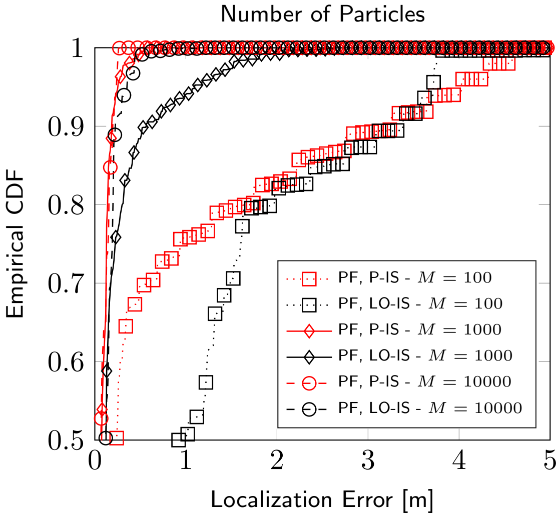

Conclusions

- We investigated a tracking problem where **large arrays** are able to elaborate the *phase profile* of an impinging waveform
- The **spherical wavefront** is exploited to estimate the state of a moving source
- The positioning information is extrapolated from the COA of the wavefront when the source is in the **near-field region**.
- Numerical results show that robust tracking performance can be obtained when exploiting only the COA encapsulated in the measured phases.

Corresponding Journal

A. Guerra, F. Guidi, D. Dardari and P. M. Djuric, "Near-field Tracking with Large Antenna Arrays: Fundamental Limits and Practical Algorithms," in IEEE Transactions on Signal Processing, doi: 10.1109/TSP.2021.3101696.

Conclusions

- We investigated a tracking problem where **large arrays** are able to elaborate the *phase profile* of an impinging waveform
- The **spherical wavefront** is exploited to estimate the state of a moving source
- The positioning information is extrapolated from the COA of the wavefront when the source is in the **near-field region**.
- Numerical results show that robust tracking performance can be obtained when exploiting only the COA encapsulated in the measured phases.

Corresponding Journal

A. Guerra, F. Guidi, D. Dardari and P. M. Djuric, "Near-field Tracking with Large Antenna Arrays: Fundamental Limits and Practical Algorithms," in IEEE Transactions on Signal Processing, doi: 10.1109/TSP.2021.3101696.

Conclusions

- We investigated a tracking problem where **large arrays** are able to elaborate the *phase profile* of an impinging waveform
- The **spherical wavefront** is exploited to estimate the state of a moving source
- The positioning information is extrapolated from the COA of the wavefront when the source is in the **near-field region**.
- Numerical results show that robust tracking performance can be obtained when exploiting only the COA encapsulated in the measured phases.

Corresponding Journal

A. Guerra, F. Guidi, D. Dardari and P. M. Djuric, "Near-field Tracking with Large Antenna Arrays: Fundamental Limits and Practical Algorithms," in IEEE Transactions on Signal Processing, doi: 10.1109/TSP.2021.3101696.

Conclusions

◇ We investigated a tracking problem where **large arrays** are able to elaborate the *phase profile* of an impinging waveform

◇ The **spherical wavefront** is exploited to estimate the state of a moving source

◇ The positioning information is extrapolated from the COA of the wavefront when the source is in the **near-field region**.

◇ Numerical results show that robust tracking performance can be obtained when exploiting only the COA encapsulated in the measured phases.

Corresponding Journal

A. Guerra, F. Guidi, D. Dardari and P. M. Djuric, "Near-field Tracking with Large Antenna Arrays: Fundamental Limits and Practical Algorithms," in IEEE Transactions on Signal Processing, doi: 10.1109/TSP.2021.3101696.

Conclusions

- We investigated a tracking problem where **large arrays** are able to elaborate the *phase profile* of an impinging waveform
- The **spherical wavefront** is exploited to estimate the state of a moving source
- The positioning information is extrapolated from the COA of the wavefront when the source is in the **near-field region**.
- Numerical results show that robust tracking performance can be obtained when exploiting only the COA encapsulated in the measured phases.

Corresponding Journal

A. Guerra, F. Guidi, D. Dardari and P. M. Djuric, "Near-field Tracking with Large Antenna Arrays: Fundamental Limits and Practical Algorithms," in IEEE Transactions on Signal Processing, doi: 10.1109/TSP.2021.3101696.